Applied Catalysis B: Environmental 92 (2009) 30–40

Contents lists available at ScienceDirect

Applied Catalysis B: Environmental

journal homepage: www.elsevier.com/locate/apcatb

Effects of sulfate species on V_2O_5/TiO_2 SCR catalysts in coal and biomass-fired systems

Xiaoyu Guo, Calvin Bartholomew, William Hecker, Larry L. Baxter *

Department of Chemical Engineering, Brigham Young University, 350 Clyde Building, Provo, UT 84602, USA

ARTICLE INFO

Article history:
Received 7 May 2009
Received in revised form 21 July 2009
Accepted 23 July 2009
Available online 3 August 2009

Keywords:
SCR catalyst
In situ FTIR
MS
XPS
Activity
Intrinsic kinetics

ABSTRACT

Sulfation occurs when commercial vanadia SCR catalysts are exposed to SO_2-laden coal combustion flue gases. Effects of sulfation on the surface chemistry of vanadia/titania catalysts and SCR activity have not been adequately addressed in previously published work. In this work, *in situ* FTIR spectroscopy and *post situ* XPS investigations were performed during vanadia/titania catalyst sulfation under simulated coal combustion flue gas conditions. *In situ* FTIR spectroscopy combined with XPS analyses on fresh and sulfated TiO_2, 2% and 5% V_2O_5/TiO_2 indicate that sulfate does not form on vanadia sites but rather on titania sites. FTIR spectroscopy data show that sulfation inhibits NO adsorption in the presence of oxygen, but greatly enhances NH_3 adsorption by generating additional Brønsted acid sites while reducing the concentration of Lewis acid sites. Observed increases in the intrinsic NO reduction activity of sulfated vanadia/titania catalysts (relative to fresh catalysts) are consistent with spectroscopy data showing that the sulfation enhances NO reduction activity by increasing the number of active sites without changing the activation energy or site acid strength.

1. Introduction

Selective catalytic reduction (SCR) of NO_x with NH_3 over vanadia/titania catalysts represents the most widely used and efficient post-combustion technique for reducing NO_x emissions from stationary combustion sources sufficient to meet stringent emission regulations. In most stationary combustion processes, SO_2 forms by oxidation of sulfur present in the fuel. SO_2 is the equilibrium sulfur species at high-temperature, oxidizing conditions. At flue gas temperatures, SO_3 is more stable than SO_2 but its formation is strongly kinetically limited. SCR catalysts designed to promote NO_x reduction to N_2 commonly also promote SO_3 formation. In a typical SCR process, SO_3 can react with the ammonia reducing agent, leading to the formation of ammonia sulfate and bisulfate. Ammonia bisulfate is an undesirable product because it forms small acidic and corrosive particles that can plug small passages in the air heater, cause fouling of the catalyst surface, and plug catalyst pores.

Surface sulfate species also form when gas-phase SO_3 interacts with SCR catalyst surface species, including vanadium and titanium oxide, or other catalyst components. Previous investigations indicate that sulfur species either enhance or reduce catalyst activity [1,2]. Brønsted acid sites, the suggested active centers, are reportedly strengthened with the formation of surface sulfates, which in turn increase and stabilize catalyst activity [3]. On the other hand, calcium sulfate, formed when sulfur oxides react with free CaO present in flyash of coal combustion processes, reportedly masks the catalyst surface and thereby deactivates the catalyst by limiting reactant gas access to the catalyst interior surface [4].

Previous investigations of SO_2 interactions with vanadia/titania catalysts have been limited in scope and accordingly fail to provide a consistent picture of the chemistry of surface sulfur species and their effects on catalytic activity. For example, there is no consensus regarding the mechanisms of formation, location, and chemical structure of SO_x (SO_2, SO_3, sulfate species) adsorbed on vanadia/titania catalysts, and how sulfate species influence active sites and catalyst activity [5,6]. Orsenigo et al. [5] compared effects of sulfation on NO_x reduction and SO_2 oxidation activities, suggesting that sulfation occurs first on vanadia sites and later on titania and tungsta sites. However, these conclusions were drawn in the absence of confirming experimental evidence from surface science methods. Dunn et al. [6], Choo et al. [7], and Amiridis et al. [8] investigated the correlation between sulfation and vanadia/titania catalyst performance; and Chen and Yang [9] investigated SCR activity on sulfated TiO_2. However, these investigations were performed either on vanadia catalysts with artificially introduced sulfate species by impregnation [6–8]; or on *in situ* sulfated TiO_2 but not vanadia catalysts [9]. It is questionable if impregnated sulfate species in the catalyst are representative of sulfate species formed during the SCR reaction in the presence of

* Corresponding author. Tel.: +1 801 422 8616; fax: +1 801 422 0151.
E-mail address: larry_baxter@byu.edu (L.L. Baxter).

0926-3373/$ – see front matter © 2009 Elsevier B.V. All rights reserved.
doi:10.1016/j.apcatb.2009.07.025

SO_2. It was also unclear from those works if surface species monitored *ex situ* are the same as those formed under *in situ* conditions.

To address the above issues, we designed and completed a systematic *in situ* experimental investigation of sulfation on vanadia/titania SCR catalyst performance. *Operando* FTIR spectroscopy was applied for monitoring surface species during sulfation, while *ex situ* XPS analyses determined elemental composition and the oxidation states on both non- and sulfated vanadia catalysts. The combination of *in situ* FTIR and *ex situ* XPS techniques reveals (1) details regarding the chemical speciation of the catalyst surface, (2) a better understanding of the effects of surface sulfate species on SCR catalyst performance, and (3) further insights into the reaction and deactivation mechanisms. Effects of catalyst sulfation on BET surface area and porosity, NH_3 and NO adsorption capacities, NO_x reduction activity, and concentration and temperature dependencies of SCR catalysts were also investigated. The results of these experiments shed new light on (1) the chemical nature of surface sulfate sites, (2) the mechanism and extent of sulfate activity enhancement of catalyst NO_x reduction activity, and (3) the SCR reaction mechanism.

2. Experimental

2.1. Catalyst preparation

Titanium dioxide (P25, Degussa) was densified by mixing with distilled water at 1:1.75 weight ratio and dried at 120 °C for 24 h followed by calcination at 600 °C for 4 h. The densified titanium dioxide was then ground with an agate mortar and pestle into a fine powder.

Vanadia/titania catalysts were prepared by incipient impregnation using ammonium metavanadate (>99.5%, Fisher Scientific) as the active component precursor to achieve nominal metal loading of 1, 2, and 5 wt.%, all of which are below monolayer coverage since monolayer coverage is reached at 6 wt.% [8]. The precursor was added in a stoichiometric ratio into a warm (50 °C) oxalic acid solution, resulting in a deep blue solution. After the precursor solution cooled down, titania powder was added to it. The slurry thus formed was dried at 120 °C for 8 h while stirring to evaporate most of the water, followed by calcination at 550 °C for 6 h. After calcination, the catalyst was ground with an agate mortar and pestle to a fine powder.

2.2. A In situ FTIR spectroscopy

Infrared spectra were obtained using a Nicolet 730 FTIR spectrometer with an MCT detector. Circular, self-supported, thin catalyst wafers with 1.5 cm diameter were prepared by pressing 80 mg of sample. The catalyst wafer was mounted in a reactor cell depicted in Fig. 1. The reactor cell allowed reactant gases to pass across both wafer surfaces. Prior to collecting spectra, samples were pretreated in a high-purity flow of 5 wt.% O_2/He at 380 °C for 2 h. The background spectrum was recorded in flowing helium and was subtracted from the sample spectrum. In the experiment, the *in situ* IR spectra were recorded by accumulating 75 scans at a spectral resolution of 2 cm^{-1}.

2.3. Surface sulfation

The sulfation was conducted on TiO_2, 2 and 5 wt.% V_2O_5/TiO_2 with a gas composition of 2700 ppm SO_2, 5% O_2, 0 or 4% water vapor, and helium. Moisture was introduced by passing purified helium through a bubbler. Sulfation was carried out at 1 atm and 380 °C. *In situ* FTIR spectra were collected during sulfation with CaF_2 and KCl windows to prevent the flowing gases from diffusing into the rest of the cell. CaF_2 was placed next to the catalyst pellet since it is inert to SO_2 and SO_3 containing gases. Additional KCl or NaCl windows also provided thermal insulation for the heated cell. CaF_2 windows were chosen for *in situ* FTIR monitoring due to their inertness to sulfation. Since, however, CaF_2 blocks IR radiation below 1100 cm^{-1}, a NaCl window was used for already-sulfated samples, since NaCl transmits IR below 1100 cm^{-1} (but above 625 cm^{-1}).

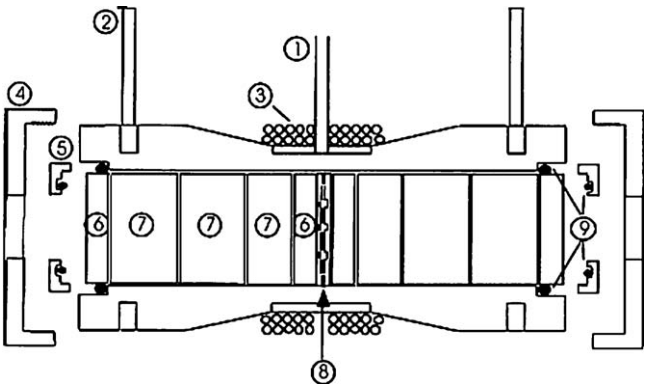

Fig. 1. Schematic diagram of the *in situ* IR reactor cell: (1) thermocouple port; (2) water cooling ports; (3) thermocoax heating cable; (4) end caps; (5) Teflon window holders; (6) CaF_2 windows; (7) KCl windows; (8) aluminum wafer holder; (9) Nitrile (large) and Kalrez (small) O-rings. Not shown are the gas inlet and outlet ports, located on either side of the reactor near (6) coming out of the page.

2.4. NH_3 and NO adsorption

Ammonia or NO adsorptions on the catalyst wafer were monitored by *in situ* FTIR spectroscopy. After pretreatment (Section 2.2), the temperature was decreased to 50 °C and room temperature for ammonia and NO adsorptions, respectively.

During NH_3 or NO adsorption, 1000 ppm NH_3 in helium (50 ml/min) or 1000 ppm NO in argon (95 ml/min) was introduced continuously for 1.0 h to ensure complete saturation of the sample. NH_3 or NO was then replaced by helium (50 ml/min) to purge the system for another hour to eliminate effects from physically adsorbed species. Subsequently, FTIR spectra were recorded. It was found that the amounts of NH_3 and NO adsorbed on the catalyst changed little before and after purging with helium.

2.5. X-ray photoelectron spectroscopy (XPS)

XPS is a surface sensitive analytical technique providing compositional data and elemental oxidation states in the outer 1–20 nm of a surface, with a minimum detection limit of 0.5 atomic %. XPS spectra were collected using an SSX-100 ESCA from an area 800 μm × 800 μm in size, using a monochromatised Al Kα (1486.7 eV) X-ray beam. All spectra were collected at a pressure of 5×10^{-9} Torr and a power consumption of 200 W. The instrument was regularly calibrated to the Au $4f_{7/2}$ peak at 84.0 eV. Spectra are charge corrected to the main line of the C 1s spectrum set to 285.0 eV. Surface elemental composition and oxidation state were calculated using XPS instrument software.

2.6. Activity measurements

Activity data were collected in the intrinsic reaction regime and are thus truly represent surface reaction kinetics with negligible impacts from film and pore diffusion. In this investigation, catalyst activity measurements were carried out on 1 wt.% V_2O_5/TiO_2 in a temperature range of 250–300 °C to ensure intrinsic kinetics. These conditions correspond to Thiele modulus (M_T) of about 0.25

(250 °C) and 0.34 (300 °C), corresponding to effectiveness factors of 0.96 and 0.93, respectively. Therefore, pore diffusion does not appreciably influence the measured rates at these temperatures for the 1 wt.% vanadia catalyst, which corresponds to the typical vanadia content of commercial SCR catalysts. In the remaining kinetic tests on vanadia catalysts (fresh and sulfated) M_T was maintained below 0.4 by adjustments of flow rate and temperature during rate measurements.

Film diffusion tests on SCR catalysts (1 wt.% V_2O_5/TiO_2) were conducted at three different flow rates (93, 121 and 187 ml/min at ambient conditions, corresponding to space velocities of 100,000, 130,000, and 200,000 h^{-1}, respectively). This range of space velocities provides a significant variation in the thickness of the boundary layer surrounding the catalyst particle and therefore should result in different conversions if film resistance plays a significant role in NO reduction. Essentially identical NO conversions obtained at 250 °C (17.6% at 93.3 ml/min, 18% at 121 ml/min, and 17.4% at 187 ml/min) are consistent with the mathematical expectation of negligible film transport resistance.

Theoretical calculation results show that film diffusion represents a trivial consideration during SCR tests on 1% V_2O_5/TiO_2 at temperatures up to 350 °C as well, i.e., it accounts for about 0.3% of the total resistance (combined film diffusion and reaction resistances). Note that the nominal composition of the vanadium oxide is by convention written as V_2O_5 (the starting oxide composition after calcination), although it is probably present as a mixture of different oxides, i.e., V_2O_x where $x = 3–5$ (oxide composition is addressed later).

Kinetic parameters were calculated directly from NO conversion based on Eqs. (1) and (2) (assuming the surface reaction is first-order in NO concentration):

$$k' = -\frac{Q_0}{W_{cat}} \ln(1 - X) \quad (1)$$

$$k' = A \exp\left(-\frac{E_a}{RT}\right) \quad (2)$$

where k' is the reaction rate coefficient (ml g^{-1} s^{-1}), Q_0 the total gas flow rate (ml min^{-1}), W_{cat} the catalyst weight (g), X the NO conversion (%), A the pre-exponential factor, E_a the activation energy (J mol^{-1}), R the gas constant (8.3145 J mol^{-1} K^{-1}) and T is the temperature (K). A matrix of reaction rate coefficients (k) and temperatures results from measuring NO conversion as a function of temperature was solved using a non-linear regression routine (Igor Pro® software) providing non-linear least-squares fits of these observed rate data with 95% confidence intervals, and values of the parameters A and E_a and their confidence intervals.

NO conversion was measured using a Balzers-Pffeiffers Prisma™ QMS 100 quadruple mass spectrometer (MS) to sample the exhaust and feed from the FTIR reactor cell using a Faraday cup and secondary electronic measuring detectors. This instrument was capable of measuring concentrations in the 1 ppm range based on MS signal intensity changes in the NO^{30}/Ar^{38} ratio between reactor feed and effluent.

3. Results and discussion

This work provides new insights into the surface chemistry and catalysis of SCR by vanadia/titania SCR catalysts, including (1) chemical structure and surface location of adsorbed sulfur, (2) chemistries of NO and NH_3 adsorptions, (3) the chemical structure and location of active sites, (4) the effects of adsorbed sulfur on active site density, and (5) catalytic roles of titania and vanadia species. Evidence for these new insights from this and previous studies is presented and discussed under the following topics ordered so as to unfold the authors' train of observations, logic and understanding.

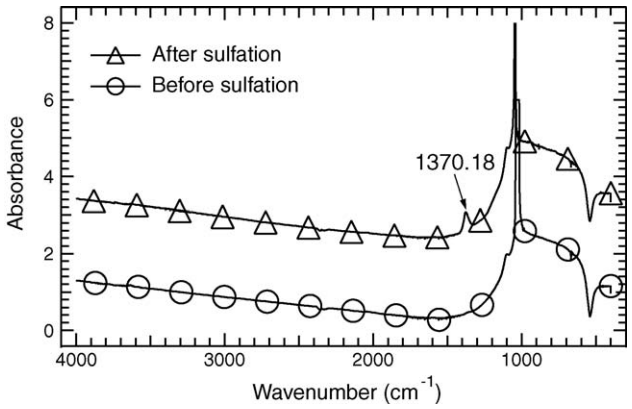

Fig. 2. IR spectra comparison of 5 wt.% V_2O_5/TiO_2: before and after sulfation with an arbitrary vertical offset (90% helium, 10% O_2, total flow rate of 50 ml/min at room temperature).

3.1. Identification of sulfur species on V_2O_5/TiO_2

3.1.1. Investigation of sulfation by in situ FTIR spectroscopy

Sulfur species formed on the catalyst surface during SO_2/O_2 exposure (sulfation) were monitored either by *in situ* or *ex situ* FTIR spectroscopy either during or before and after sulfation treatments. Fig. 2 compares the *ex situ* IR spectra of fresh and 24-h sulfated 5 wt.% vanadia catalyst with an arbitrary vertical offset. These two spectra were collected in helium with NaCl windows at room temperature.

The only observable difference between the two spectra is a peak near 1370 cm^{-1} for the sulfated catalyst, which is assigned to the S=O stretching of sulfate species on SCR catalysts [6,7,10,11]. The broad peak at 1100–700 cm^{-1} is assigned to an overtone mode of vanadia [12]. Formation of sulfate species on the vanadia catalyst does not seem to interfere with the overtone IR peak of vanadia because neither the shape nor the intensity of overtone peak changes. The observation of only one relevant peak at 1370 cm^{-1} using NaCl windows indicates that CaF_2 cell windows used in *in situ* measurements and which eliminate the region below 1100 cm^{-1} do not block valuable information during *in situ* FTIR spectroscopy monitoring of the sulfation.

In situ FTIR spectra of pure TiO_2, 2 and 5 wt.% V_2O_5/TiO_2 were collected during sulfation at 380 °C under both dry and moist conditions. A sulfate peak at 1375 cm^{-1} appears about 10–30 min after the introduction of SO_2/O_2 for both TiO_2 and V_2O_5/TiO_2 catalysts. Sample purging following sulfation was conducted for 1–2 h with helium at 380 °C. The ~1375 cm^{-1} peak remained at the same intensity during this purging, indicating that sulfate species, rather than other adsorbed sulfur species, are formed on sample surfaces.

3.1.1.1. Sulfation of TiO_2. *In situ* FTIR spectra collected during TiO_2 sulfation under dry (TiO_2–O) and moist (TiO_2–H) conditions appear in Figs. 3 and 4, respectively, with vertical offsets showing effects of exposure time. (Offsets in these and later figures do not indicate changes in absorbance.) It appears that sulfate peak intensity is largely constant after about 5–6 h. Nevertheless, shifts in peak position were observed up to 24 h. Results of a previous study suggest that sulfation is complete after 24 h [5].

Spectra for sulfated TiO_2 (dry and wet—Figs. 3 and 4) consist of a doublet with peaks of roughly equal intensity at 1367–1381 and 1386–1408 cm^{-1}, respectively. Doublet IR intensity increases gradually with time for both dry and wet samples (Figs. 3 and 4); moreover, peak positions shift to higher frequencies with increasing time during the sulfation test, indicating increasing sulfate acidity with time/surface coverage. In addition, the sulfate

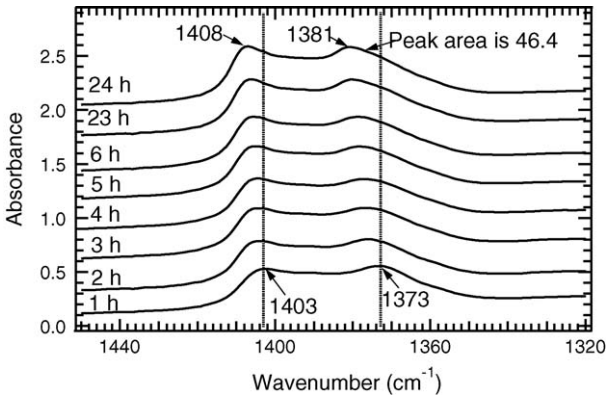

Fig. 3. Time-dependent, *in situ* FTIR spectra of titania exposed to 2700 ppm SO_2, 5% O_2, helium balance, at 380 °C.

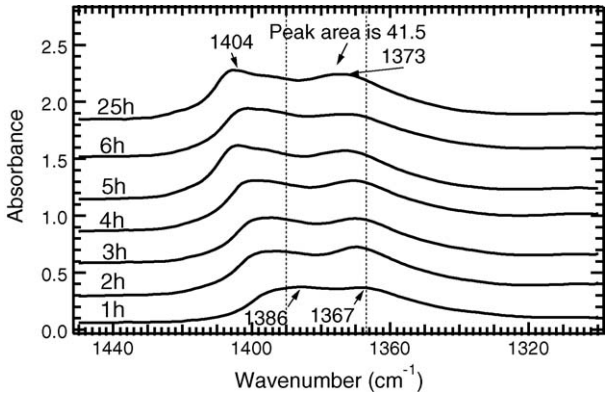

Fig. 4. Time-dependent, *in situ* FTIR spectra of titania exposed to 2700 ppm SO_2, 5% O_2, helium balance, with water vapor at 380 °C.

peak area after 24 h is greater for the dry sample relative to the wet sample (relative area of 46 versus 41).

A doublet peak was also reported in Yang et al.'s work for sulfated TiO_2 [11], for which the peak around 1380 cm^{-1} was reportedly more intense than the one around 1401 cm^{-1}. On the other hand, our results, show that the peak around 1401 cm^{-1} is only slightly more intense for titania, while it nearly disappears in vanadia/titania samples.

3.1.1.2. Sulfation of 2 and 5 wt.% V_2O_5/TiO_2. In situ FTIR spectra collected during sulfation of 2 wt.% V_2O_5/TiO_2 under dry and moist conditions are shown in Figs. 5 and 6, respectively. The spectra

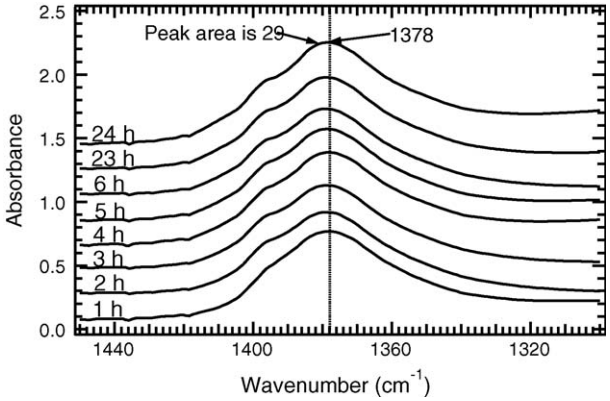

Fig. 5. Time-dependent, *in situ* FTIR spectra of a 2 wt.% V_2O_5/TiO_2 catalyst exposed to 2700 ppm SO_2, 5% O_2, helium balance, at 380 °C.

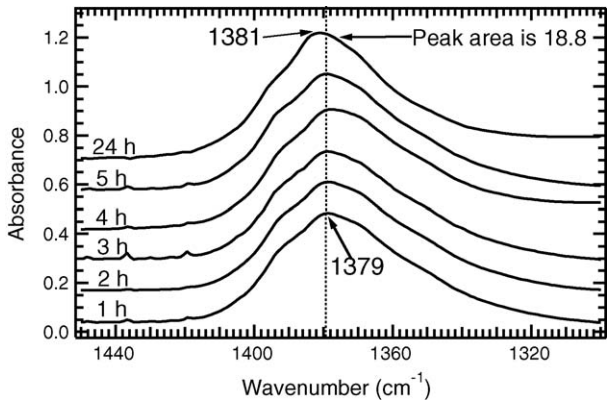

Fig. 6. Time-dependent, *in situ* FTIR spectra of a 2 wt.% V_2O_5/TiO_2 catalyst exposed to 2700 ppm SO_2, 5% O_2, helium balance, with water vapor at 380 °C.

show only minor evidence of a doublet with a weak shoulder peak at ~1400 cm^{-1} and an intense major peak at ~1380 cm^{-1}. The sulfate peak intensities and positions are constant over time for both dry and wet sulfations after about 4 h. Therefore, sulfation reaches completion more rapidly on 2 wt.% V_2O_5/TiO_2 (within about 4 h) than on pure titania (within about 24 h). The peak areas for sulfated 2 wt.% V_2O_5/TiO_2, 29 for dry and 19 wet sulfation, are smaller than the areas observed for titania samples (46 for dry and 42 for wet). As observed for titania, the IR peak area for 2 wt.% V_2O_5/TiO_2 is larger during dry sulfation (29) than during wet sulfation (19).

The *in situ* FTIR spectra collected during sulfation of 5 wt.% V_2O_5/TiO_2 under dry and moist conditions (Figs. 7 and 8, respectively) reveal a single, low-intensity IR peak around 1369 cm^{-1}, the area of which is substantially smaller after wet sulfation (3.9 versus 17.3). Due to the weak intensity of the sulfate peak formed during wet sulfation (Fig. 8), effects of background noise are evident in these spectra. Sulfation occurs rapidly (within 1 h) on 5 wt.% V_2O_5/TiO_2; i.e., sulfate peak intensities and positions for 5 wt.% V_2O_5/TiO_2 (dry and wet) remain the same from the first hour to the 24th hour. Thus, sulfation of 5 wt.% V_2O_5/TiO_2 occurs more rapidly and results in the smallest sulfate peak among 0, 2 and 5 wt.% V_2O_5/TiO_2 under either dry or wet conditions.

Comparing sulfate peaks formed on pure TiO_2, 2 and 5 wt.% V_2O_5/TiO_2, it is evident that as vanadia content is increased, the doublet (peaks at 1400 and 1380 cm^{-1} in the case of TiO_2) transforms to a singlet at 1380 cm^{-1} accompanied by a shoulder around 1400 cm^{-1} (for 2 wt.% V_2O_5/TiO_2) to a singlet at 1380 cm^{-1} with no shoulder (for 5 wt.% V_2O_5/TiO_2). Moreover, as vanadia content increases the IR wavenumber of the sulfate peak shifts

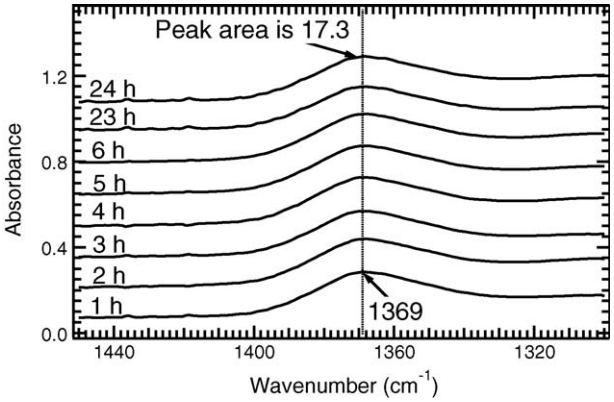

Fig. 7. Time-dependent, *in situ* FTIR spectra of a 5 wt.% V_2O_5/TiO_2 catalyst exposed to 2700 ppm SO_2, 5% O_2, helium balance, at 380 °C.

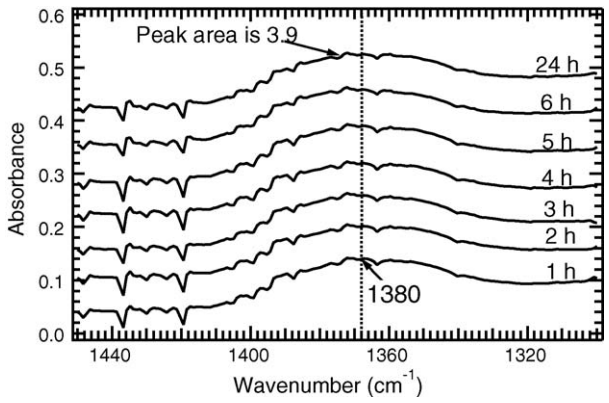

Fig. 8. Time-dependent, *in situ* FTIR spectra of a 5 wt.% V_2O_5/TiO_2 catalyst exposed to 2700 ppm SO_2, 5% O_2, helium balance, with water vapor at 380 °C.

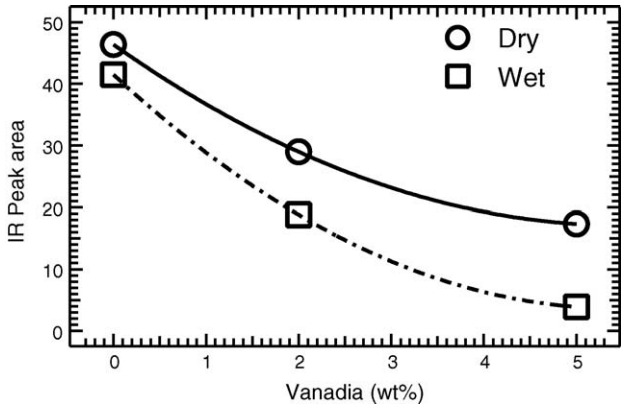

Fig. 9. FTIR sulfate peak area of V_2O_5/TiO_2 versus vanadia loading for both dry (○) and wet (□) conditions.

slightly to lower wavenumber values, *while sulfate peak area substantially decreases for both wet and dry samples* (see Fig. 9), a clear indication that the extent of sulfation decreases with increasing vanadia content and with addition of moisture. Thus, based on the trends in Fig. 9, *we conclude that vanadia sulfates significantly less than titania, if at all*, since by extrapolation the IR peak area should approach zero at high vanadia content. Moreover, it appears that vanadia species may occupy surface sulfation sites on TiO_2, which are possibly surface hydroxyl group [13], leading to a decrease in the number of available sulfation sites in 5 wt.% V_2O_5/TiO_2.

3.1.2. Investigation of sulfation by XPS

Results of XPS analyses for TiO_2 and V_2O_5/TiO_2 with 2 and 5 wt.% V_2O_5 after 24-h exposure to dilute SO_2/O_2 in the absence and presence of water vapor (two replicates each) are summarized in Table 1. Ti, V, and O binding energies from the literature for TiO_2, sulfated TiO_2, and VO_x (dry and wet, unsupported and TiO_2-supported) are summarized in Table 2 and compared with data from this study; O binding energies for O–V, O–H and O–C are also included.

In the catalyst of this study (Table 1), C, O, S, V and Ti are observed to be the principal elements on the surface of TiO_2 and V_2O_5/TiO_2 catalysts. Carbon contamination of catalyst surfaces at 10% level is typical, probably resulting from (1) carbon impurities originally in TiO_2, (2) hydrocarbon contaminants from the air adsorbed on the catalyst during storage of calcined samples and their transfer to the XPS system, and (3) hydrocarbon precursors used in catalyst preparation. The BE of the C 1s of 285.0 serves as reference for our XPS data.

Ti $2p_{2/3}$ binding energies of 458.2–458.4 eV following dry sulfation (this study) are near values of 458.4–458.8 for unsulfated Ti^{4+} in TiO_2 (see Table 2) while that for TiO_2 following sulfation with water vapor of 459.5 eV is higher than highly sulfated TiO_2 (459.1 eV) with sulfuric acid, respectively [15]. BEs for either dry- or wet-sulfated 2 and 5 wt.% V_2O_5/TiO_2 of 458.2 and 458.7 eV are not higher than values of 458.7 and 458.5 eV for fresh 2 and 5 wt.% V_2O_5/TiO_2, respectively, indicating less pronounced sulfation impact on titania species on vanadia/titania catalysts than on titania support alone. Nevertheless, the XPS Ti $2p_{2/3}$ binding energy (BE) data of this study after wet sulfation show the same trend of increasing BE with increasing extent of sulfation for TiO_2 and V_2O_5/TiO_2 (i.e. 458.2, 458.7, 459.5 eV for 5 wt.% V_2O_5/TiO_2, 2 wt.% V_2O_5/TiO_2, and TiO_2), respectively as observed by Jung and Grange [15] for TiO_2 sulfated with sulfuric acid.

V $2p_{2/3}$ binding energies of 516.4–517.2 eV following sulfation of 2 and 5 wt.% V_2O_5/TiO_2 (this study) are near values reported for V^{4+} and V^{5+} in 2 wt.% V_2O_5/TiO_2 (see Table 2), suggesting that vanadium in the sulfated V_2O_5/TiO_2 catalysts of this study consists of a mixture of IV and V oxidation states. The BE of 516.4 eV for dry-sulfated 2 wt.% V_2O_5/TiO_2 is also close to the upper value of 516.2 eV for $VOSO_4$ and the value of 516.3 eV for VO_2; nevertheless,

Table 1
XPS results from two replicates for TiO_2 and V_2O_5/TiO_2 with 2 and 5 wt.% vanadia loadings. Sulfation conditions: 2700 ppm SO_2, 5% O_2, helium balance, at 380 °C, with or without water vapor.

After dry sulfation				After sulfation with water			
Sample	Elements[a]	BE[b]	Atom %[c]	Sample	Element	BE	Atom %
TiO_2	C 1s	285.0	8.7	TiO_2	C 1s	285.0	10.2
	O 1s	529.5	66.4		O 1s	530.5	70.7
	S 2p	168.5	2.8		S 2p	169.5	3.4
	Ti $2p_{3/2}$	458.4	23.2		Ti $2p_{3/2}$	459.5	15.6
2 wt.% V_2O_5	C 1s	285.0	8.3	2 wt.% V_2O_5	C 1s	285.0	10.1
	O 1s	533.7	67.7		O 1s	530.6	65.2
	S 2p	169.0	2.1		S 2p	169.3	2.4
	Ti 2p	458.2	20.9		Ti 2p	458.7	20.2
	V $2p_{3/2}$	516.4	1.9		V $2p_{3/2}$	517.2	2.1
5 wt.% V_2O_5	C 1s	285.0	24.2	5 wt.% V_2O_5	C 1s	285.0	5.3
	O 1s	534.0	56		O 1s	533.4	65.8
	S 2p	168.5	1.5		S 2p	168.6	2.8
	Ti $2p_{3/2}$	458.2	16.5		Ti $2p_{3/2}$	458.2	20.2
	V $2p_{3/2}$	516.7	3.3		V $2p_{3/2}$	516.7	3.3

[a] Element and its electronic orbital.
[b] Binding energy (eV).
[c] XPS atomic percentage.

Table 2
Ti $2p_{3/2}$, V $2p_{3/2}$, O 1s, and S 2p XPS binding energies reported for vanadium oxides (unsupported and TiO_2-supported, wet and dry), vanadyl sulfate, TiO_2, and sulfated TiO_2).

Sample	BE (eV)				Ref. source
	Ti $2p_{3/2}$	V $2p_{3/2}$	O 1s	S 2p	
TiO_2	458.8		529.9		Hong et al. [14]
TiO_2[a]	458.6		529.6	168.5	Chen and Yang [9]
TiO_2	458.6		529.9		Jung and Grange [15]
1.5 wt.% SO_4/TiO_2[b]	458.9		530.1	168.9	Jung and Grange [15]
3.0 wt.% SO_4/TiO_2[b]	459.0		530.2	168.9	Jung and Grange [15]
6.6 wt.% SO_4/TiO_2[b]	459.1		530.3	169.0	Jung and Grange [15]
V oxides		515.5–517.5			XPS handbook [16]
V_2O_3 (V^{3+})		515.6 (max) ± 0.3			Bondarenka et al. [17]
V_2O_4 (dry oxide) (V^{4+})		516.5 (max) ± 0.3	529.3		Bondarenka et al. [17]
		516.3			Haber [18]
V_2O_4 (C–O or H–O bonded)			531.8		Bondarenka et al. [17]
V_2O_4 (wet oxide)			533.8		Bondarenka et al. [17]
VO_2 (V^{4+})		516.3			Haber [18]
V_2O_5 (V^{5+})		516.8–517.6			XPS handbook [16]
V_2O_5 (dry oxide) (V^{5+})		517.25 (max) ± 0.35	530.1		Bondarenka et al. [17]
V_2O_5 (C–O or H–O bonded)			532.2		Bondarenka et al. [17]
V_2O_5 (wet oxide)			533.9		Bondarenka et al. [17]
2 wt.% V_2O_x/TiO_2	456.3 (Ti^{2+})	515.1 (V^{3+})			Hong et al. [14]
Same catalyst	457.9 (Ti^{3+})	516.1 (V^{4+})			Hong et al. [14]
Same catalyst	458.8 (Ti^{4+})	517.2 (V^{5+})	529.9 (V–O)		Hong et al. [14]
	459.4				Haber [18]
Wet 2 wt.% VO_x/TiO_2			530.2 (V–OH)		Hong et al. [14]
C–O or H–O in 2 wt.% VO_x/TiO_2			531.6 (C–O)		Hong et al. [14]
TiO_2 dry, sulfated[c]	458.4		529.5	168.5	This study
TiO_2 wet, sulfated[c]	459.5		530.5	169.5	This study
TiO_2, fresh	458.4		529.4	NA	This study
2 wt.% V_2O_x/TiO_2 dry, sulfated[b]	458.2	516.4	533.7	169.0	This study
2 wt.% V_2O_x/TiO_2 wet, sulfated[b]	458.7	517.2	530.6	169.2	This study
2 wt.% V_2O_x/TiO_2, fresh	458.7	516.3	529.8	NA	This study
5 wt.% V_2O_x/TiO_2 dry, sulfated[b]	458.2	516.7	534.0	168.5	This study
5 wt.% V_2O_x/TiO_2 wet, sulfated[b]	458.2	516.7	533.4	168.6	This study
5 wt.% V_2O_x/TiO_2, fresh	458.5	516.6	530.0	NA	This study
$VOSO_4$		515.7–516.2	530.0		XPS handbook [16]
$VOSO_4$ mesoporous		516.2		168.2	Kohiki et al. [19]

[a] Sulfation with 500 ppm SO_2, 2% O_2 in N_2, 400 °C, with or without 1000 ppm NH_3 and NO, 8% H_2O, 1.5 h.
[b] Sulfation with H_2SO_4 (0.1N) at RT followed by drying 12 h at 100 °C and calcining at 5 h at 500 °C.
[c] Sulfation with 2700 ppm SO_2, 5 wt.% O_2, and He at 380 °C with or without water vapor.

the V $2p_{2/3}$ BEs for the other three samples of this study are significantly higher than the value for $VOSO_4$, suggesting that *vanadyl sulfate is not likely to be present in these samples*.

The quantity of oxygen (56–70 atom %) in the sulfated TiO_2 samples of this study (Table 1) is consistent with the presence of TiO_2, SO_4^{2-}, V_2O_5, and oxygen-containing carbon compounds (e.g., carbonyl groups) at the surface. The O 1s BE for dry-sulfated TiO_2 of 529.5 eV (this work) is close to the value (529.4 eV) of fresh TiO_2 from this study, although somewhat lower than, the value of 529.9 reported for unsulfated TiO_2 [15] (Table 2) while that of 530.5 for wet-sulfated TiO_2 is slightly higher than the value of 530.2 reported [15] for sulfuric-acid-treated TiO_2 containing 3.0 wt.% SO_4^{2-} and for hydroxyl groups on TiO_2 [14]. The O 1s BE for wet-sulfated TiO_2 can be independently estimated using the atom percentages from Table 1 and assuming CO_2, SO_4, TiO_2 and OH are the components whose oxygen content adds to 70.7% and by summing the percentages of each component times the component BE from Table 2, i.e., $(1/0.707) \times [2(0.102)(532.3) + 4(0.034)(5302.) + 2(0.156) \times (529.9) + 0.055(532.3)] = 530.8$ eV, a value in fairly good agreement with 530.5 eV; note that 5.5 wt.% OH used for the last term of this calculation was determined from the difference between 70.7% (overall percentage of oxygen) and the sum of expected contributions based on measured percentages for C, S, and Ti present as CO_2, SO_4, and TiO_2.

Values of the O 1s BE for V_2O_5/TiO_2 catalysts of this study are, with the exception of the value of 530.6 eV for wet-sulfated 2 wt.% V_2O_5/TiO_2, in the range of 533.4–534.0 eV, characteristic of wet V_2O_5, V_2O_4, or C–O or H–O bonds in 2 wt.% V_2O_5/TiO_2 but clearly substantially higher than the value of 530.0 reported for $VOSO_4$ (see Table 2). *Thus, the vanadium phase in the sulfated V_2O_X/TiO_2 catalysts of this study appears to be an oxide containing V^{4+} and V^{5+}, largely free of sulfur* and possibly bonded to OH–, C–O_X–, or H– groups.

The sulfur S 2p BEs of all six sulfated samples of this study, ranging over 168.5–169.5 eV (Tables 1 and 2), are clearly *characteristic of sulfur species present on the TiO_2 surface as S(VI) sulfates at different coverage* as reported by Jung and Grange [15]. The lower BEs for dry sulfation of 168.5–169.0 are characteristic of low sulfur coverages, while the higher BEs for wet-sulfated TiO_2 and 2 wt.% V_2O_5/TiO_2 of 169.5 and 169.2 eV are consistent with high and moderately high sulfur coverages [15]. This result corroborates the *in situ* FTIR spectral data showing a single sulfate species to be present in the catalyst following sulfation. The BEs for the sulfated samples of this study (168.5–169.5 eV) are also uniformly significantly higher than the value of 168.2 reported for $VOSO_4$ [19] *indicating that $VOSO_4$ is probably not formed, i.e., vanadium oxide is not sulfated under the conditions of this study*.

Thus, it is surmised from the comparison of the Ti, V, O, and S XPS BE data of this study (Tables 1 and 2) with those from previous studies (Table 2), that *wet exposure of TiO_2 and V_2O_5/TiO_2 catalysts to SO_2 at* 380 °C *produces a state of surface sulfation very similar chemically to that using impregnation of TiO_2 with sulfuric acid followed by drying and calcination* [15].

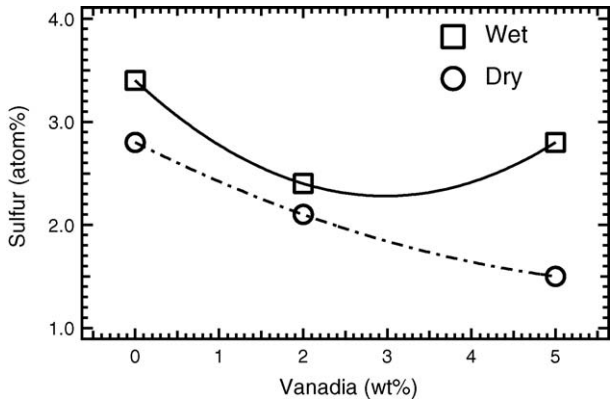

Fig. 10. Sulfur content determined by XPS after: (○) dry and (□) wet sulfation on V_2O_5/TiO_2 containing 0, 2 and 5 wt.% vanadia.

Sulfate content of wet and dry titania and V_2O_5/TiO_2 catalysts as determined from XPS analyses (Table 1) is plotted versus vanadia concentration in Fig. 10. Surface sulfate concentrations are significant for all six samples. *A trend of linearly decreasing sulfate coverage with increasing vanadium content is apparent* for samples sulfated in the absence and presence of water vapor (with the exception of a slight upturn in sulfur content for the sample of highest vanadium content generated with moist gas; this datum point was replicated, producing the same result). The overall trend agrees with that from *in situ* FTIR spectra showing that the intensity of the IR peak at 1370–1375 cm^{-1} for sulfate decreases with increasing vanadia content of the catalyst. *Together, the XPS and FTIR data of this study* (Figs. 9 and 10 *and* Tables 1 and 2), *when extrapolated to high V_2O_X content, provide evidence that sulfates are formed largely on TiO_2 and not on the vanadium oxide phase.*

3.1.3. Discussion/interpretation of FTIR and XPS results

Roles of V and Ti phases in sulfate formation. Together, the XPS and *in situ* FTIR spectral results of this work, showing a trend of decreasing sulfate formation with increasing vanadium content, indicate that (1) TiO_2 species are much more readily sulfated than vanadia species and (2) possibly no sulfate is formed on the vanadia phase in V_2O_5/TiO_2 catalysts during exposure to SO_2/O_2 at 380 °C. Similar trends of decreasing FTIR sulfate peak intensity with increasing vanadia concentration were observed in previous non-*in situ* studies [6,8,20]. Dunn et al. [6] found that (1) the molecular structure of the surface vanadia species is only slightly perturbed by the presence of sulfur and (2) surface sulfate species adsorb on basic support hydroxyl species. Both these conclusions are consistent with those of this study. Choo et al. [7] claimed that surface vanadate species titrate both basic and neutral support hydroxyls, forming a complete, close-packed monolayer, thereby explaining the decrease in sulfation capacity with increasing vanadium content. In other words, vanadia and sulfate species occupy the same surface group, the hydroxyls group associated with titania. With higher vanadia content, less hydroxyl group is available on titania for sulfation to occur.

Since sulfation of TiO_2 by SO_2 must involve an increase in the oxidation state of sulfur, catalysis of SO_2 oxidation to SO_3 by V_2O_5 followed by adsorption on a TiO_2–OH site to produce a sulfate could well play an important role in this process. Vanadium oxide is a well-known catalyst for SO_2 oxidation to SO_3. The presence of mobile V^{5+} species and water vapor would probably greatly facilitate this conversion (see discussion of mobility below). It is apparent from the kinetic data of this study (Figs. 4–8) that sulfation occurs more rapidly on V_2O_5/TiO_2 relative to TiO_2; indeed, the catalyzed sulfation by vanadia species and less available Ti–OH group on vanadia catalyst results in a rate of sulfation in the order TiO_2 < 2 wt.% V_2O_5/TiO_2 < 5 wt.% V_2O_5/TiO_2 (although the extent of sulfation progresses in the opposite order). Thus, catalysis of SO_2 oxidation to SO_3 by vanadium oxide is consistent with these results. Therefore, vanadia species contribute to faster SO_2 oxidation, but the extent of sulfation is determined by the available Ti–OH group left from the consumption by the vanadia species.

Orsenigo et al. [5] compared sulfation of an SCR catalyst during NO_x reduction and SO_2 oxidation, concluding that sulfation occurs first on vanadia sites and later on titania. This conclusion, however, was based on macroscopic observations and not on specific surface analyses of sulfation sites on SCR catalysts as in the previously cited IR and XPS studies and this comprehensive FTIR/XPS investigation. Their conclusion is probably correct to the extent that vanadia probably does catalyze the SO_2 oxidation, the first step in the process. However, the surface science (this and previous IR and XPS studies) largely supports the view that while SO_3 is formed on vanadia, it desorbs from vanadia and adsorbs to the titania surface to form a sulfate.

Effects of water on extent of sulfation; *resolution of an apparent discrepancy*. Effects of water on the extent of sulfation appear to be different for FTIR and XPS methods, i.e., the significantly higher surface sulfur content from XPS for the samples sulfated in the presence of water vapor (Fig. 10) suggests that water promotes accumulation of sulfur on both TiO_2 and V_2O_5/TiO_2 catalysts. This observation is contrary to that observed for the same catalysts by FTIR spectroscopy (see Fig. 9) suggesting that water reduces accumulation of sulfur on TiO_2 and V_2O_5/TiO_2 catalysts as reflected by a weaker sulfate IR peak.

The weaker IR peak intensities for the wet samples are likely a result of adsorbed water causing the intensity of the sulfate peak to diminish. In fact, it was observed in this study that the 1375 cm^{-1} sulfate peak disappears when a sulfated vanadia/titania catalyst is exposed to water vapor at 375 °C in helium in the absence of gas-phase SO_2, and reappears after dehydration with no further SO_2 introduction. Thus, water apparently diminishes the IR intensity of the sulfate peaks for these samples at this wavenumber without actually removing sulfate. The most probable reason for the change in peak intensity could be that water forms hydrated sulfates on the surface, altering the vibration modes relative to the original sulfate. Based on isotope exchange and IR data [11,21], previous investigators suggested that the tridentate structure of the dry sulfate on the titania surface [$(M–O)_3S{=}O$] changes to a bridge bidentate [$(M_2SO_4)H$] structure under wet conditions as shown in Scheme 1. This hypothesis is consistent with the decrease in intensity of the 1375 cm^{-1} sulfate peak observed after water addition, i.e., the decrease in peak area is due to the change in bonding of the sulfur from a double S=O bond to hybrid S–O_2H bond.

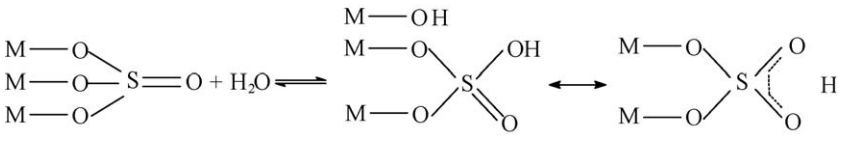

Scheme 1. Change in the sulfate structure due to hydration [21].

Role of water vapor and surface migration in promoting sulfate formation. The XPS data (Fig. 10) indicate that sulfate formation on TiO_2 and the TiO_2 phase of V_2O_5/TiO_2 catalysts occurs to a greater extent in the presence of water vapor; this is especially true of TiO_2 and 5 wt.% V_2O_5/TiO_2. This behavior may relate to the effects of water vapor on (1) surface structure of catalytic phases; (2) surface dynamics, e.g. migration, of participating catalytic phases; and (3) hydroxylation of TiO_2 and V_2O_x surfaces.

An example of water inducing structural changes in metal sulfates is presented and discussed immediately above and illustrated in Scheme 1. A possible consequence of water-induced structural changes might be formation of highly porous or non-wetting surface vanadia structures which could lead to greater access of the underlying TiO_2 sites for sulfate formation. Observations of vanadium oxide monomer or dimer clusters on dilute V_2O_5/TiO_2 catalysts, e.g. 1% V_2O_5/TiO_2, and of polymeric or crystallite oxide forms at higher vanadia loadings have been well documented [22–24]. While the effects of water vapor on these structures has not been well documented, it is reasonable to conclude that effects of water would vary with vanadia loading, thus explaining the varying magnitudes of sulfation for wet relative to dry conditions as a function of vanadia loading evident in Fig. 10. For example, at relatively high vanadia concentrations (e.g., 5 wt.%), it may become easier for the vanadia species to agglomerate in the presence of water, thus allowing new titania surface sites to be exposed for adsorption of SO_2 or SO_3 and producing a higher sulfate concentration represented by an upturn of wet-sulfated 5 wt.% V_2O_5/TiO_2.

Enhanced migration of surface species in the presence of water vapor is a well-known phenomenon in sintering of catalysts and formation of new surface phases, e.g. formation of metal silicates from silica-supported metals in Fischer–Tropsch synthesis [25]. Vanadia species may have significant mobility on TiO_2 or other oxide surfaces under reaction conditions depending on oxidation state, surface structure, and water vapor concentration [26–30]. In fact, dynamic properties of supported vanadia species have been shown to depend on moisture content and temperature [30]. Moreover, supported metal oxide atoms begin to diffuse significantly when temperature rises above its Tammann temperature ($T_{TAM} = \sim(1/2)T_{MP}$ where T_{MP} is the metal oxide melting point) [13,31]. The Tammann temperature of supported vanadia and the melting point for V_2O_5 are 209 and 690 °C, respectively. Thus, under typical SCR conditions (250–450 °C), surface V^{5+} or V^{4+} species would probably be mobile. The addition of water vapor could facilitate structural changes in vanadium oxides species that enhance their mobility, facilitating access of adsorbing molecules to the underlying TiO_2 surface. Water vapor would probably also increase surface hydroxyl concentration on TiO_2 and the probability of SO_2 or SO_3 adsorption thereon.

3.2. Impact of sulfation on BET surface area and pore diameter

Surface area and mean pore size for fresh and fully sulfated 1% V_2O_5/TiO_2 catalyst are summarized in Table 3. 24-h sulfation decreases the surface area of 1% V_2O_5/TiO_2 by 16%, and increases the corresponding average pore diameter by about 10%. Those relatively minor variations indicate that sulfation lowers catalyst surface area slightly but significantly within the experimental error of the adsorption measurements.

Table 3
BET surface area and average pore diameter of fresh and 24-h dry-sulfated 1% V_2O_5/TiO_2.

	1% V_2O_5/TiO_2[a]	24-h sulfated 1% V_2O_5/TiO_2[a]
BET surface area (m^2/g)	25.2 ± 0.1	21.1 ± 0.1
Mean pore size (nm)	41.4 ± 2.0	45.8 ± 2.0

[a] With three replicates.

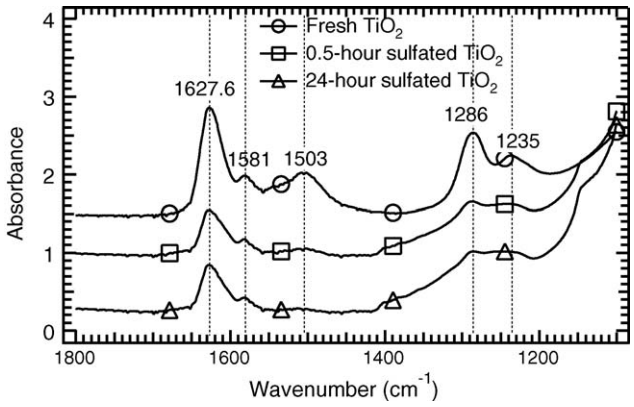

Fig. 11. NO adsorption on TiO_2 at RT with various degrees of sulfation (1000 ppm NO, 10% O_2, helium balance, total flow rate of 95 ml/min).

3.3. Impact of sulfation on NO adsorption

In the presence of 1000 ppm NO in argon only, no adsorption occurs on TiO_2 or vanadia catalysts at 25 °C, as monitored by *in situ* FTIR spectroscopy. However, when TiO_2 and 1% V_2O_5/TiO_2 catalysts were exposed to 10% oxygen and 1000 ppm NO/argon, optically detectable IR peaks were observed in the range of 1620–1220 cm^{-1} (see Figs. 11 and 12). Indeed, intense peaks arise at 1628, 1581, 1503, 1286, 1235 cm^{-1} on TiO_2, and at 1622, 1574, 1502, 1285, 1222 cm^{-1} on 1% V_2O_5/TiO_2. These peaks can be assigned to three different bridging and chelating nitrate species [20,32,33]. Additionally, 1 wt.% addition of V_2O_5 on TiO_2 surface downshifts the wavenumbers of nitrate species.

Nitrate species also form on sulfated TiO_2 and 1% V_2O_5/TiO_2, but at lower concentrations. Indeed, nitrate species peak intensity decreases with increasing extent of sulfation (Figs. 11 and 12). For both TiO_2 and 1% V_2O_5/TiO_2, the 1500 cm^{-1} peak is apparently the most sensitive absorption band, as its intensity decreases substantially upon sulfation or addition of V_2O_5 and disappears entirely after 24 h of sulfation.

The observed decrease in nitrate peak intensity and shift to higher wavenumbers in its peak position upon addition of 1% vanadia and the decrease in nitrate peak intensity due to sulfation suggest that (1) surface vanadia may weaken the bonds between the nitrate and the catalyst surface and (2) both sulfate and vanadia species compete with NO for surface hydroxyl groups on the TiO_2 surface. No observable NO absorption occurs above room temperature.

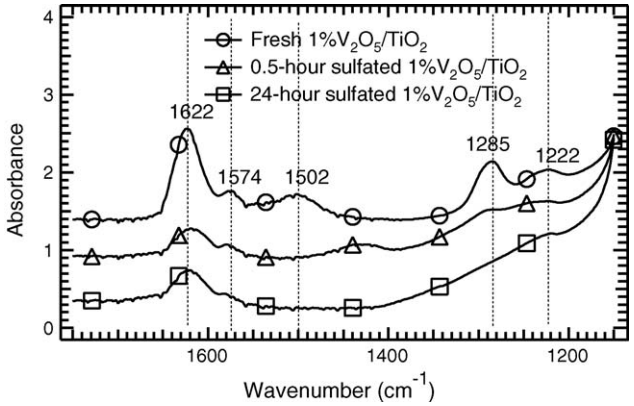

Fig. 12. NO adsorption on 1% V_2O_5/TiO_2 at RT with various degrees of sulfation (1000 ppm NO, 10% O_2, helium balance, total flow rate of 95 ml/min).

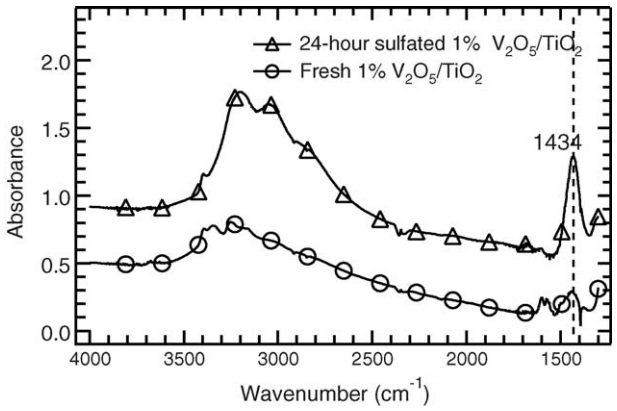

Fig. 13. NH_3 adsorption on fresh, lightly sulfated, and 24-h sulfated 1% V_2O_5/TiO_2 at 50 °C (1000 ppm NH_3, helium balance, total flow rate of 50 ml/min).

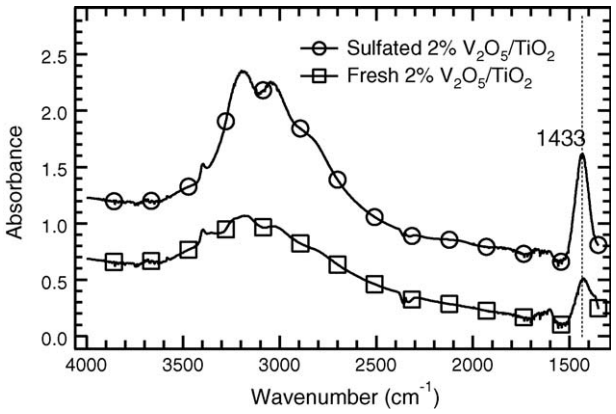

Fig. 14. NH_3 adsorption on fresh and 24-h sulfated 2 wt.% V_2O_5/TiO_2 at 50 °C (1000 ppm NH_3, helium balance, total flow rate of 50 ml/min).

The lack of NO adsorption in the absence of gas-phase oxygen indicates that oxygen plays an important role in the oxidation of NO, probably to NO_2, enabling the adsorption of NO_2 on titania-hydroxyl groups to produce a surface nitrate. However, it appears that the nitrate is either not formed or a spectator species under reaction conditions; rather, during reaction gas-phase NO_2 produced by oxidation of NO is more likely to react with adsorbed ammonia to form an intermediate that decompose to N_2 [2,12].

3.4. Impact of sulfation on NH_3 adsorption on 1, 2, and 5 wt.% V_2O_5/TiO_2

Ammonia adsorption was observed by *in situ* FTIR on non-sulfated and sulfated vanadia catalysts at 50 °C. Data in Fig. 13 show that significant quantities of ammonia adsorb on fresh and sulfated 1% V_2O_5/TiO_2. Two major adsorbed ammonia peaks appear on fresh 1% V_2O_5/TiO_2, as shown in Fig. 13. The peak at 1601 cm^{-1} corresponds to ammonia coordinatively adsorbed on Lewis acid sites, while that at 1440 cm^{-1} arises from ammonia chemisorbed on Brønsted acid sites [34]. After 24-h exposure of 1% V_2O_5/TiO_2 to SO_2, the intensity of the peak at 1440 cm^{-1} corresponding to chemisorbed ammonia increases substantially while the intensity of the peak at 1601 cm^{-1} greatly decreases, to the point of being negligible.

Areas of the peak at 1440 cm^{-1} for fresh and sulfated 1% V_2O_5/TiO_2 are summarized in Table 4. Sulfation enhances ammonia adsorption on Brønsted acid sites, that is, after only 30 min of sulfation, ammonia adsorption on Brønsted acid sites increases by 150%, and after 24-h sulfation by 350%. Thus, sulfation apparently reduces the number of Lewis acid sites, and increases the number but not the acid strength of Brønsted acid sites on the titania surface, i.e., the IR peak frequency is the same before and after sulfation. Accordingly, it is also possible that sulfate species transforms Lewis acid sites into Brønsted acid sites on the titania surface.

For NH_3 adsorbed on 2 and 5 wt.% V_2O_5/TiO_2 catalysts (Figs. 14 and 15), IR peak intensities for Lewis acid sites (at 1601 cm^{-1}) are essentially negligible, while peak intensities for Brønsted acid sites (1433 cm^{-1}) are very significant and increase substantially after

Table 4
1434 cm^{-1} IR peak areas for fresh, lightly sulfated, and 24-h sulfated 1% V_2O_5/TiO_2 at 20 °C.

Sulfation degree	Fresh	30-min sulfation	24-h sulfation
1433 cm^{-1} peak area	11.3	25.9	50.8
Peak area increase		150%	350%

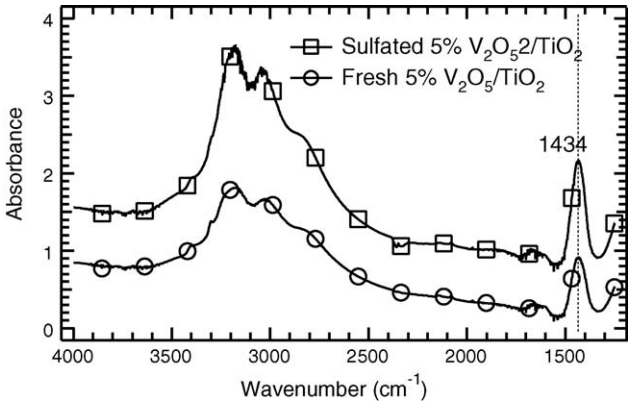

Fig. 15. NH_3 adsorption on fresh and 24-h sulfated 5 wt.% V_2O_5/TiO_2 at 50 °C (1000 ppm NH_3, helium balance, total flow rate of 50 ml/min).

sulfation. For instance, the IR peak areas at 1433 cm^{-1} increased by 350, 100, and 75 wt.% on 1, 2, and 5 wt.% V_2O_5/TiO_2, respectively, after 24-h sulfation. These results further confirm that surface sulfate species reduce the number of Lewis acid sites and increase the number of Brønsted acid sites. However, the strength of Brønsted acid sites remains unchanged, i.e., the ammonia adsorption peak wavenumber remains constant upon sulfation. The relative enhancement of ammonia adsorption by sulfation is progressively smaller with increasing vanadia content, consistent with a lower extent of sulfation with increasing vanadia content.

3.5. Impact of sulfation on NO_x reduction activity

Plots of NO kinetic rate constants versus temperature appear in Fig. 16 for fully (24-h) sulfated, lightly (30-min) sulfated, and fresh 1% V_2O_5/TiO_2 SCR catalysts. These constants were obtained from non-linear least-squares fits of rate versus temperature data collected from 250 to 290 °C. The solid lines represent the curve fits based on the non-linear least-squares analyses for each conversion data set. The upper and lower dotted lines indicate the 95 wt.% confidence interval for activity (k) at a given temperature. These results indicate that differences observed among the samples are statistically significant. Typically, sulfation increases intrinsic activity by about 40% after 30-min sulfation, and around 200% after 24-h sulfation.

Pre-exponential factors and activation energies determined from non-linear regression appear in Table 5. Significantly larger pre-exponential factors are observed for sulfated samples ($A = 5.8 \times 10^5$ and 3.0×10^5 $cm^3/g\,s$) relative to fresh samples

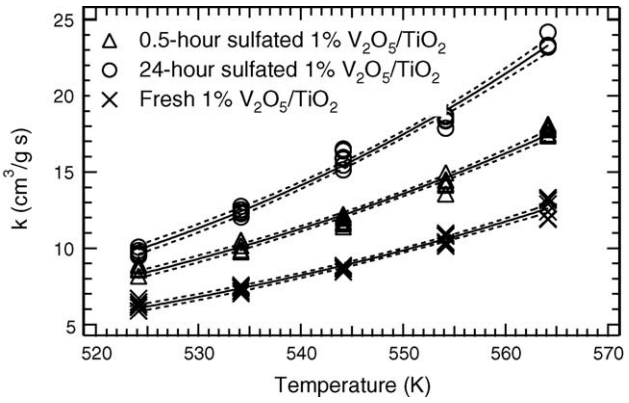

Fig. 16. Kinetic rate constant comparisons with confidence intervals of fresh, lightly sulfated, and 24-h sulfated 1% V_2O_5/TiO_2, and fresh 1% V_2O_5–9% WO_3/TiO_2 at temperatures from 200 to 300 °C.

Table 5
Kinetic parameter (A, E_a) comparisons of fresh, lightly sulfated, and 24-h sulfated 1% V_2O_5/TiO_2.

	24-h sulfated 1% V/TiO_2	0.5-h sulfated 1% V/TiO_2	Fresh 1% V/TiO_2
A	$5.8 \times 10^5 \pm 1.1 \times 10^5$	$3.0 \times 10^5 \pm 1.1 \times 10^5$	$1.8 \times 10^5 \pm 1.5 \times 10^5$
% increase	322	166	
E_a	$4.8 \times 10^4 \pm 3.5 \times 10^3$	$4.6 \times 10^4 \pm 3.5 \times 10^3$	$4.5 \times 10^4 \pm 3.5 \times 10^3$

($A = 1.8 \times 10^5$ cm^3/g s) while activation energy (E_a = 45–48 kJ/mol) is constant within experimental error among the three samples. The percentage increase in pre-exponential factors agrees well with increases in the number of Brønsted acid sites with sulfation.

Thus, the enhanced kinetic rates for sulfated samples are due to a larger pre-exponential factor, which conceptually scales with the number of the active sites. The constant activation energy, on the other hand, indicates that the same reaction mechanism operates for unsulfated and sulfated samples.

3.6. Discussion/interpretation of adsorption and activity results

The results of this work, viewed in the context of FTIR and XPS studies of sulfation, FTIR studies of NO and NH_3 adsorptions on sulfated materials, intrinsic activity measurements as a function of the extent of sulfation, and of previous relevant studies, provide new insights into the surface chemistry and mechanisms of adsorption and reaction processes during SCR on V_2O_x/TiO_2.

Adsorption of reactants. The IR NO adsorption results of this work, showing that gas-phase oxygen is necessary for surface nitrate formation, suggests that nitrates are likely formed by oxidation of NO to NO_2 followed by adsorption of NO_2 on an Ti–OH site on the catalyst. That surface nitrate formation is attenuated by either sulfate or vanadium addition to the catalyst and that both sulfates and vanadia adsorb to TiO_2–OH sites, indicates that surface nitrates are probably formed competitively on these same sites. Under reaction conditions, nitrate formation is probably not important in SCR, since previous mechanistic work [2,12] provides evidence that during reaction gas-phase NO_2 reacts directly with adsorbed ammonia or ammonium ions.

The NH_3 IR adsorption experiments of this study provide evidence that sulfation substantially increases Brønsted acid site density, while decreasing Lewis acid site density. Moreover, the increase in SCR catalytic activity due to sulfation correlates well with the increase in Brønsted acid site density, indicating that Brønsted sites contribute, probably dominantly, to the active sites for reaction. A good correlation was obtained by comparing sulfation impact on NH_3 adsorption and SCR reaction kinetic parameters: the percentage of accumulated Brønsted acid sites (150 and 350%) is consistent with the degree of pre-exponential factors enlargement (166 and 322%); unchanged acidity of Brønsted acid sites is indicated by with same SCR reaction activation energy before and after sulfation. This correlation strongly suggests a mechanism in which sulfation enhances vanadia/titania catalyst SCR activity by introducing more active Brønsted acid sites without enhancing the acidity or changing the reaction mechanism. The IR/XPS data of this and previous studies showing that sulfates are formed mainly on TiO_2, further identifies the TiO_2 surface as the source of active acid sites for NH_3 adsorption.

Active sites in SCR. The spectral data of this and of previous studies also implicate V_2O_x sites in the oxidation of SO_2 to SO_3 followed by formation of the sulfate on TiO_2. The ability of vanadium to readily undergo changes in oxidation state (differences in binding energy between oxidation states of III, IV, and V are small—see Table 2), enables it to act as a reducing or oxidizing medium. Thus, proposed mechanisms for SCR typically involve either oxidation or reduction of NO by V_2O_x/TiO_2. For example, Topsøe et al. [2] postulated an SCR catalytic cycle involving two sites where NH_3 first adsorbs on a Brønsted acid site, V–OH, which acts in conjunction with an oxidation-state shift of a V=O site (+4 to +5) to reduce gas-phase NO.

However, the results of this work show that Brønsted acid sites are not limited to V–OH and might also involve S–OH group. The evidence cited earlier regarding high mobility of vanadium ions during reaction supports a model involving oxidation of NO to NO_2 on V^{5+} followed by gas-phase reaction of NO_2 with ammonia adsorbed on the Brønsted acid sites (V–OH and S–OH). Given the previously discussed potential for mobility of vanadium and hydroxyl ions under high-temperature reaction conditions (350–400 °C) in the presence of a high water partial pressure, it follows that SO_3 could form on a vanadium site and could easily hop or migrate to neighboring Ti–OH sites and form an S–OH group. This dual-site behavior explains the necessity of having both vanadium and titanium oxides present in a high-activity catalyst.

While Orsenigo et al. [5] reported only a short-term (few hours) enhancement of NO_x reduction with sulfation followed by an increasing evolution of SO_3 at the exit of their reactor, our comprehensive investigation indicates that sulfation enhances NO_x reduction activity in both short (0.5 h) and long terms (24 h).

Correlations between the electronic structure and surface acidity of TiO_2–SO_4^{2-} with different SO_4^{2-}amounts were investigated by means of NH_3-TPD, NH_3-FTIR and XPS in a previous study [15]. BEs of O 1s in hydroxyls and Ti $2p_{2/3}$ were found to increase with increasing sulfate loading. A linear relation was obtained between Ti 2p binding energy shift and Lewis acid sites, while the shift in O 1s binding energy was attributed both to the generation of NH_3 hydrogen bond and of Brønsted acid sites. These results are consistent with the IR and XPS data of this study and provide evidence that the ammonia adsorption sites are correlated with a decrease in electron density of O 1s in hydroxyl (Brønsted type and H bonded) and Ti $2p_{2/3}$ (Lewis type) by the inductive influence of a neighboring sulfate ion [15].

4. Conclusions

1. *In situ* FTIR and XPS studies of 0, 2, and 5 wt.% V_2O_5/TiO_2 sulfation provide evidence that stable sulfate species are formed on titania, but not on vanadia.
2. Water vapor enhances titania sulfation suggesting that sulfation is formed by interaction of SO_2 with hydroxyl groups on the titania surface.
3. IR data show that O_2 is necessary for NO adsorbed on titania and V_2O_5/TiO_2 and create surface nitrate species. The intensity of nitrate species decreases with increasing extent of sulfation.

4. Ammonia is adsorbed on both Brønsted and Lewis acid sites, both of which are IR active. The density of Brønsted acid sites increases and that of Lewis acid sites decreases with increasing extent of sulfation.
5. Sulfation does not change the acidity of Brønsted acid sites.
6. SCR activation energy obtained from this study is about 45 kJ/mol.
7. The intrinsic rate of SCR of 1% V_2O_5/TiO_2 at 250–290 °C increases by about 40% after sulfation for 30 min and about 200% after sulfation for 24 h.
8. Brønsted acid sites primarily effect SCR catalysis. Sulfation enhances intrinsic SCR activity of 1% V_2O_5/TiO_2. The enhancement quantitatively appears as an increase of the pre-exponential factor and no change in the activation energy, indicating an increased number of Brønsted acid sites and no change in acidity.
9. Sulfation enhancement mechanism: sulfation enhances vanadia/titania SCR activity by introducing additional Brønsted acid sites without affecting the acidity of Brønsted acid sites.
10. Surface Brønsted acid sites come not only from surface V–OH group, but could also from surface S–OH group.

Acknowledgments

We would like to acknowledge the support of Department of Chemical Engineering at Brigham Young University, and support from Aaron Nackos.

References

[1] J.P. Chen, R.T. Yang, J. Catal. 125 (1990) 411–420.
[2] N.Y. Topsøe, J.A. Dumesic, H. Topsoe, J. Catal. 151 (1995) 241–252.
[3] R. Khodayari, C.U.I. Odenbrand, Appl. Catal. B: Environ. 33 (2001) 277–291.
[4] K. Rigby, R. Johnson, R. Neufert, G. Pajonk, E. Hums, A. Klatt, R. Sigling, in: Proceedings of 2000 International Joint Power Generation Conference, Miami Beach, Florida, 2000.
[5] C. Orsenigo, L. Lietti, E. Tronconi, P. Forzatti, F. Bregani, Ind. Eng. Chem. Res. 37 (1998) 2350–2359.
[6] J.P. Dunn, J.-M. Jehng, D.S. Kim, L.E. Briand, H.G. Stenger, I.E. Wachs, J. Phys. Chem. B 102 (1998) 6212–6218.
[7] S.T. Choo, Y.G. Lee, I.-S. Nam, S.-W. Ham, J.-B. Lee, Appl. Catal. A: Gen. 200 (2000) 177–188.
[8] M.D. Amiridis, I.E. Wachs, G. Deo, J.M. Jehng, D.S. Kim, J. Catal. 161 (1996) 247–253.
[9] J.P. Chen, R.T. Yang, J. Catal. 139 (1993) 277–288.
[10] S.M. Jung, P. Grange, Catal. Today 59 (2000) 305–312.
[11] R.T. Yang, W.B. Li, N. Chen, Appl. Catal. A: Gen. 169 (1998) 215–225.
[12] N.Y. Topsøe, H. Topsoe, Catal. Today 9 (1991) 77–82.
[13] I.E. Wachs, Y. Chen, J.-M. Jehng, L.E. Briand, T. Tanaka, Catal. Today 78 (2003) 13–24.
[14] S.-H. Hong, S.-J. Hong, S.-C. Hong, T.-S. Park, J.-Y. Lee, Vanadium/Titania-based Catalyst for Removing Nitrogen Oxide at Low Temperature Window, and Process of Removing Nitrogen Oxide Using the Same, Int. Patent No. WO 2005/030389 A1, Korea, 2005.
[15] S.M. Jung, P. Grange, Catal. Lett. 76 (2001) 27–30.
[16] J.F. Moulder, W.F. Stricle, P.E. Sobol, K.D. Bomben, Handbook of X-ray Photoelectron Spectroscopy, Perkin-Elmer Corporation, Physical Electronics Division, 1995 .
[17] V. Bondarenka, S. Grebinskij, S. Mickevicius, H. Tvardauskas, S. Kaciulis, V. Volkov, G. Zakharova, A. Pasiskevicius, Lithuanian J. Phys. 47 (2007) 333–342.
[18] J. Haber, Catal. Today 142 (2009) 100–113.
[19] S. Kohiki, H. Shimooka, S. Takada, A. Shimizu, T. Hirakawa, S. Takahashi, H. Deguchi, M. Oku, Chem. Lett. (2002) 670–671.
[20] G. Ramis, G. Busca, Appl. Catal. 64 (1990) 243–257.
[21] O. Saur, M. Bensitel, A.B.M. Saad, J.C. Lavalley, C.P. Tripp, B.A. Morrow, J. Catal. 99 (1986) 104–110.
[22] U.S. Ozkan, Y. Cai, M.W. Kumthekar, J. Phys. Chem. 99 (1995) 2363–2371.
[23] G.T. Went, L.J. Leu, A.T. Bell, J. Catal. 134 (1992) 479–491.
[24] G.T. Went, L.J. Leu, S.J. Lombardo, A.T. Bell, J. Phys. Chem. 96 (1992) 2235–2241.
[25] C.H. Bartholomew, R.J. Farrauto, Fundamentals of Industrial Catalytic Processes, 2nd ed., John Wiley & Sons Inc., Hoboken, New Jersey, 2006.
[26] L.E. Briand, O.P. Tkachenko, M. Guraya, X. Gao, I.E. Wachs, W. Gruenert, J. Phys. Chem. B 108 (2004) 4823–4830.
[27] I.E. Wachs, Catalysis 13 (1997) 37–54.
[28] I.E. Wachs, Catal. Today 100 (2005) 79–94.
[29] I.E. Wachs, B.M. Weckhuysen, Appl. Catal. A-Gen. 157 (1997) 67–90.
[30] I.E. Wachs, B.M. Weckhuysen, Appl. Catal. A: Gen. 157 (1997) 67–90.
[31] C.-B. Wang, C.Y.I.E. Wachs, Langmuir 15 (1999) 1223.
[32] K. Hadjiivanov, Catal. Rev.: Sci. Eng. 42 (2000) 71–144.
[33] G. Ramis, G. Busca, F. Bregani, P. Forzatti, Appl. Catal. 64 (1990) 259–278.
[34] D.A. Pena, Development and Characterization of Mixed Oxide Catalysts for the Selective Catalytic Reduction of Nitric Oxide from Stationary Sources Using Ammonia Chemical Engineering, University of Cincinnati, Cincinnati, OH, USA, 2003, p. 266.